IEEE Access
Multidisciplinary | Rapid Review | Open Access Journal

Received December 5, 2020, accepted December 25, 2020, date of publication January 5, 2021, date of current version January 19, 2021.

Digital Object Identifier 10.1109/ACCESS.2021.3049435

Partial Discharge Signal Extraction Method Based on EDSSV and Low Rank RBF Neural Network

XIAOLI YANG[1], HONGGUANG HUANG[1], QIN SHU[1], (Member, IEEE), DAKUN ZHANG[2], AND BOJIAN CHEN[3]

[1]School of Electrical Engineering and Information, Sichuan University, Chengdu 610065, China
[2]Chengdu Ruichi Technology Company Ltd., Chengdu 610023, China
[3]State Grid Fujian Electric Power Research Institute, Fuzhou 350007, China

Corresponding author: Hongguang Huang (hhg11@163.com)

ABSTRACT The detection process of partial discharge (PD) ultra-high frequency (UHF) signal is easily affected by white noise and periodic narrowband noise, which hinder the fault diagnosis of high-voltage electrical appliances. In order to extract PD UHF signal and suppress noise effectively, this paper provides a new method to detect PD UHF signal by EDSSV and low rank RBF neural network. Firstly, the singular value decomposition (SVD) is performed on the mixed noises of PD signal. Secondly, the peak index of energy difference spectrum of singular value (EDSSV) is selected as optimal singular value threshold, and then the periodic narrowband noise is eliminated by reconstructing the effective rank order. Finally, radial basis function (RBF) neural network is used to approximate the denoised PD signal, and Gaussian window filter is used to extract the PD signal. To verify the performance of the proposed method, we compared it with other three algorithms in simulation and field detection, including adaptive singular value decomposition (ASVD), singular value decomposition based on S-transform and MTFM (S-SVD) and EMD-WT algorithms. Particularly, four evaluation indices are designed for the detection data, which consider both the noise suppression and feature preservation. The results demonstrate the validity of the proposed method with higher signal-to-noise ratio and less waveform distortion.

INDEX TERMS PD signal, singular value decomposition, energy difference spectrum of singular value, neural network, noise reduction, Gaussian window.

I. INTRODUCTION

Insulation fault of gas insulated switchgear (GIS) will seriously affect safe operation of power grid [1]. In general, partial discharge (PD) is the precursor and main cause of equipment insulation deterioration. Therefore, the insulation state of the equipment can be evaluated by partial discharge [2], [3]. Due to its advantages such as high detection sensitivity and strong anti-interference ability, UHF detection method is widely used in the detection of partial discharge in GIS [4]. The field detection environment is accompanied by various background noise, among which Gaussian white noise and the periodic narrowband noise are the most serious [5], [6]. Ultra-high frequency (UHF) signals generated by PD are extremely weak and easy to be covered by noise, which greatly increases the difficulty of PD UHF signal detection. Therefore, a reliable noise suppression method is the premise of PD signal accurate detection and diagnosis.

At present, a variety of methods have been proposed on noise suppression of PD signals, the common methods are wavelet transform (WT) [7], [8], empirical modal decomposition (EMD) [9], [10], and singular value decomposition (SVD) [11]. The WT features good time-frequency analysis ability. But it is difficult to select the optimal wavelet basis for signal decomposition, and its wavelet basis function and decomposition scale have great influence on denoising effect. Unlike the wavelet method, the EMD method derives the basic functions from the signal itself. It adaptively decomposes signal into multiple modal components, which shows good robustness. However, when the frequency of each component is relatively close, modal aliasing tends to occur, leading to the failure of denoising. Moreover, singular value decomposition (SVD) as a new signal analysis method has been utilized for noise suppression [12], [13], but the order of effective singular values needs to be determined artificially

The associate editor coordinating the review of this manuscript and approving it for publication was Chengpeng Hao.

[13], thus human factors have a great impact on the denoising effect. In recent years, the radical basis function (RBF) neural network has been applied in partial discharge pattern recognition by some scholars due to its advantages such as simple structure, fast learning speed and strong nonlinear approximation ability [14], [15]. However, this method has not been used in the research of denoising.

In this paper, a novel denoising method based on EDSSV and low-rank RBF neural network (EDSSV-RBF) is proposed. Energy difference spectrum of singular value (EDSSV) is an adaptive method to select the effective singular value, which overcomes the difficulties in determining the effective rank order, thus realizes narrowband noise suppression. Furthermore, the low-rank RBF neural network approximates the PD signal with preliminary noise reduction, extracts the main information of PD signal pulse, and combines the Gaussian window filtering to realize the suppression of white noise, and finally extracts the relatively pure PD signal. Through simulation and field measurement analysis, and comparing with other denoising methods, the results illustrate that the proposed method can suppress background noise in the PD UHF signal effectively.

II. SIMULATED PD SIGNAL

In engineering practice, most measured PD signals are oscillation exponential attenuated type signals [6]. Therefore, we use the single exponential decaying oscillation D_1 and double exponential decaying oscillation D_2 to simulate the PD signal:

$$D_1 = A_1 e^{-t/\tau} \sin(2\pi f_c t) \tag{1}$$

$$D_2 = A_2 \left(e^{-1.3t/\tau} - e^{-2.2t/\tau} \right) \sin(2\pi f_c t) \tag{2}$$

where A_1 and A_2 are respectively the amplitude coefficient of PD signal, τ stand for the attenuation coefficient, f_c is the oscillation frequency. Table 1 shows the detail parameters of the four PD pulses, in which I and III are single-exponential attenuated oscillating pulses, and II and IV are double-exponential attenuated oscillating pulses. In the simulation, N is 2000 and the simulated sampling frequency of each pulse is 5GSa/s. The original PD signal is shown in Fig.1(a).

However, there are various kinds of noise in the field environment. In order to simulate the field test environment, the random white noise of -2dB is superimposed on the original PD signal, and the noisy signal is shown in Fig.1(b).

Periodic narrowband noise is mainly generated by carrier communication and mobile phone communication, which can express by the superposition of sinusoidal signals of different frequencies [1], that is:

$$C = A_i \sum_{i=1}^{3} \sin(2\pi f_i t) \tag{3}$$

where the signal amplitude is set as $A_i = 1mV$, based on the frequencies of wireless communication signals in China, f_i is the narrowband noise frequency, which is set as $f_1 =$ 470MHz, $f_2 =$ 900MHz and $f_3 =$ 1800MHz [4], respectively. When superimposed with periodic narrowband noise, the mixed PD signal and its spectrum are shown in Fig.1(c) and (d). It can be seen from Fig.1(c) that PD signal is completely overwhelmed in the noise.

TABLE 1. Parameters of the simulated UHF PD signals.

PD pulse sequence	I	II	III	IV
A/mV	2	7	2	7
f_c/MHz	600	600	600	600
τ / ns	3	2	5	3

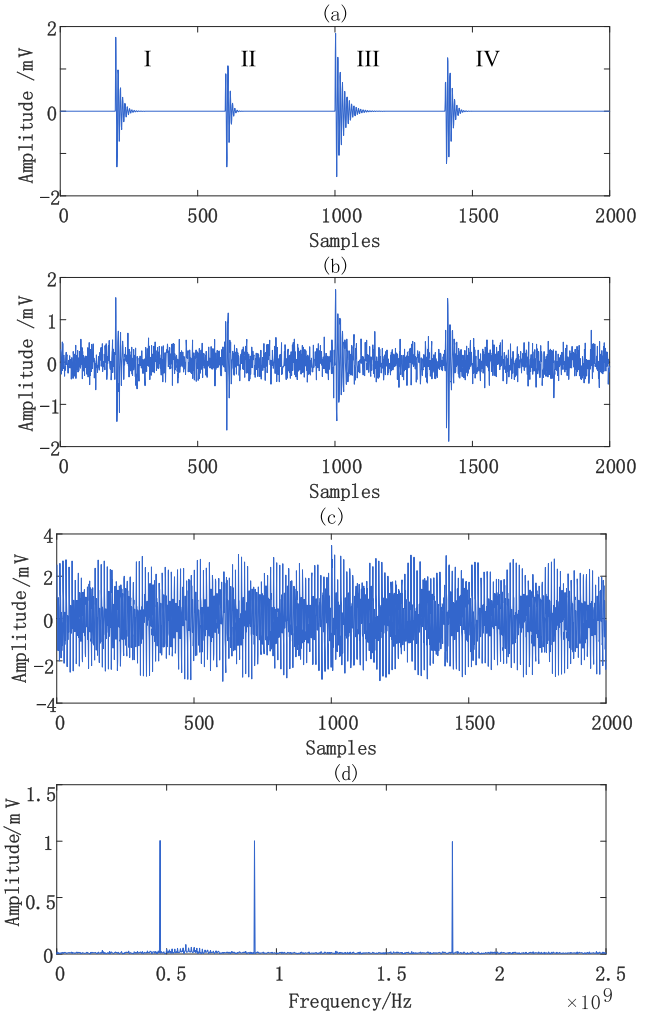

FIGURE 1. Simulated UHF PD signal and its spectrum: (a) Pure signal; (b) Noisy signal; (c) Mixed signal; (d) Spectrum of the mixed signal.

III. METHOD OF PERIODIC NARROWBAND NOISE SUPPRESSION

A. PRINCIPLE OF NARROWBAND NOISE SUPPRESSION

In general, periodic narrowband noise, white noise and PD signal are independent of each other, and the energy of periodic narrowband noise is much larger than that of PD signal and white noise [11]. The irrelevance is represented

by the orthogonality between signals. SVD can decompose the measured signals into different orthogonal components, and the singular value represents the energy of the component signals. After the singular value decomposition, the singular value of narrowband noise is obviously greater than that of other signal components, and there are significant differences between the adjacent singular values. Then the noise signal and the valid signal can be distinguished from the singular value. Therefore, in this paper, the energy difference spectrum of singular value is used to determine the threshold value and reduce noise.

1) SINGULAR VALUE DECOMPOSITION

Suppose the one-dimensional sampling sequence of mixed PD signal: $X = \{x(1), x(2), \cdots x(N)\}$, where N is sampling points. Let the sampling sequence is constructed as Hankel matrix, and the matrix decomposed by SVD. The Hankel matrix is constructed as:

$$H_{m\times k} = \begin{bmatrix} x(1) & x(2) & \cdots & x(k) \\ x(2) & x(3) & \cdots & x(k+1) \\ \vdots & \vdots & & \vdots \\ x(m) & x(m+1) & \cdots & x(N) \end{bmatrix} \tag{4}$$

where $k = N - m + 1$, and $m = N/3$. By SVD:

$$H = U\Sigma V^T \tag{5}$$

where U and V are *m-order* and *n-order* orthogonal matrix respectively, and $\sum \in \mathbb{R}^{m\times k}$ is diagonal matrix: $diag\,(\delta_1, \delta_2, \cdots \delta_s)$, where $s = \min(m, k)$ and the singular values $\{\delta_i\}_{i=1,\cdots,s}$ are arranged in descending order, namely $\delta_1 > \delta_2 > \cdots > \delta_s$.

2) DETERMINE THE EFFECTIVE SINGULAR VALUES

In signal reconstruction procedure, the key problem is to find the effective rank order $r(1 \le r < s)$ corresponding to the singular value of useful signals. If the order r is selected too small, some useful signals are considered as noise signals and removed, resulting in the loss of useful components. If the order r is too large, the reconstructed signal contains residual noise, which lead the low *SNR*. Therefore, the best effective rank order is to distinguish the useful signal and the noise accurately, so that the useful signal is retained and the noise is filtered. Due to the singular value corresponding to narrowband noise is much greater than that relating to PD signal and white noise, there is a big fluctuation in the peak position of the energy difference spectrum. Further, we can search the peak position as the effective rank order to reconstruct the narrowband noise, thereby eliminating the narrowband noise from the mixed PD signal.

The energy difference spectrum of singular value is defined and normalized [16]:

$$P(r) = \frac{\delta_r^2 - \delta_{r+1}^2}{E} \tag{6}$$

where E is the energy of singular value: $E = \sum_{r=1}^{s} \delta_r^2$.

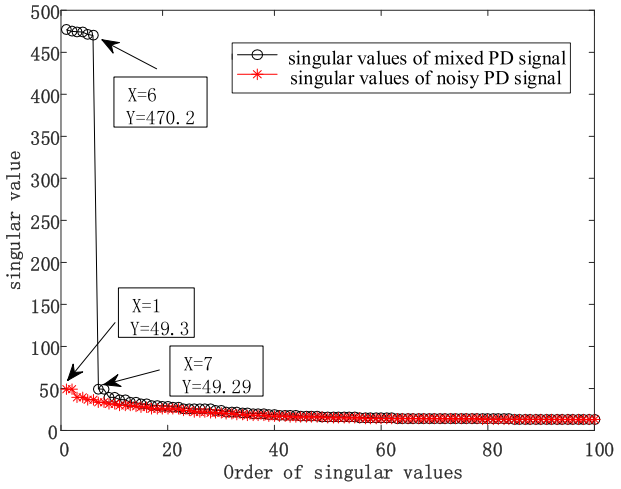

FIGURE 2. Variation curve of singular values.

The peak index of the energy difference spectrum is taken as the reconstruction order n of singular values, and the reconstructing matrix of narrowband noise is as follows:

$$X' = U_{m\times n}\Sigma_{n\times n}V_{k\times n}^T \tag{7}$$

To obtain the one-dimensional effective signal matrix, take the average value of the anti-diagonal elements of X'.

B. ENERGY DIFFERENCE SPECTRAL OF SINGULAR VALUE NOISE REDUCTION

The signals in Fig.1(b) and (c) are decomposed by SVD respectively. Further, we can obtain 666 singular values. To facilitate observation, the first 100 singular values are used for analysis. The data in Fig.2 shows obviously different in the sixth singular value and the seventh singular value due to narrowband noise. Comparing the singular value distribution of noisy PD signal, we can find that the first six singular values are correspond to the narrowband noise.

Energy difference spectrum of the singular value in Fig.2 is shown in Fig.3. It is easily seen from Fig.3 that an obvious peak appears at the sixth singular value, which also is the boundary point between useful signal and noise. Therefore, the rank order of singular values corresponding to narrowband noise can be selected automatically. Narrowband noise will be completely extracted by reconstructing the first six singular values. The reconstructed signal and frequency spectrum are shown in Fig.4. It can be seen from Fig.4(b) that after singular value decomposition and reconstruction, the three main frequencies of narrowband noise $f_1 = 470$MHz, $f_2 = 900$MHz and $f_3 = 1800$MHz have been well extracted.

C. NARROWBAND NOISE SUPPRESSION

The specific steps to suppress narrowband noise are as follows:

Step 1: Decompose the measured PD signal by SVD.

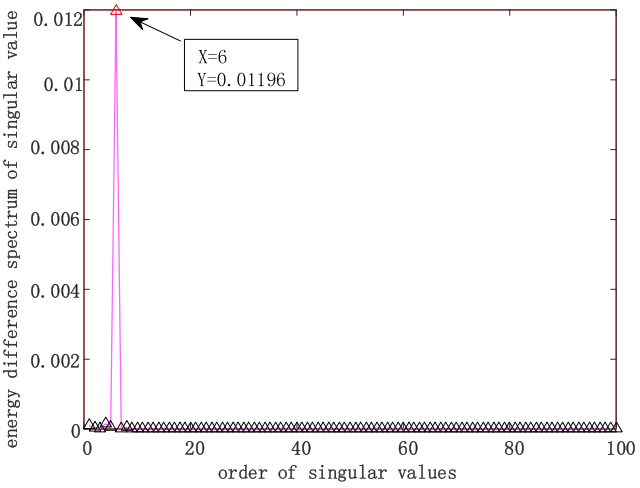

FIGURE 3. The curve of EDSSV of mixed signal.

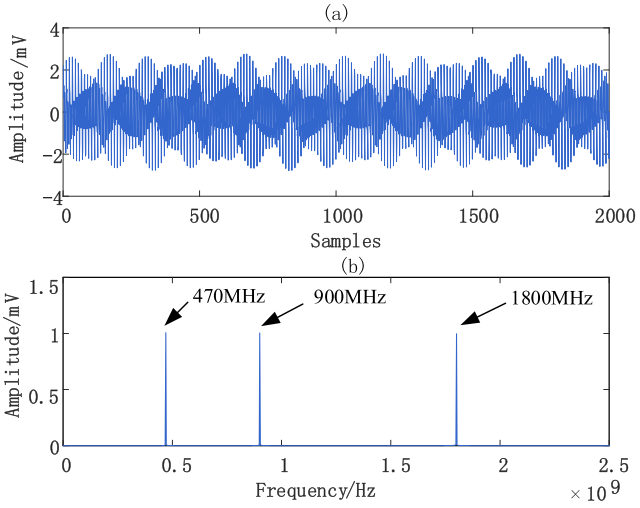

FIGURE 4. (a) Reconstructed signal and its (b) spectrum of reconstructed signal.

Step 2: Compute the energy difference spectrum of singular values, and find its peak position as the effective order number to reconstruct narrowband noise.

Step 3: Remove the reconstructed signal from the measured signal, so as to suppress periodic narrowband noise.

From the above steps, the signal in Fig.1(c) is denoised, and the denoised signal and its spectrum are shown in Fig.5. Fig.5(b) shows that the narrowband noise is eliminated successfully, which indicates that the EDSSV algorithm can accurately distinguish the singular values of useful signals and noise, and suppress the narrowband noise. Another interesting result is that the residual noise is Gaussian white noise after the narrowband noise suppressed.

IV. DENOISING METHOD OF GAUSSIAN WHITE NOISE

In order to further suppress the remaining Gaussian white noise and improve the accuracy of spectrum analysis, the pure PD signals are effectively extracted by using the Gaussian

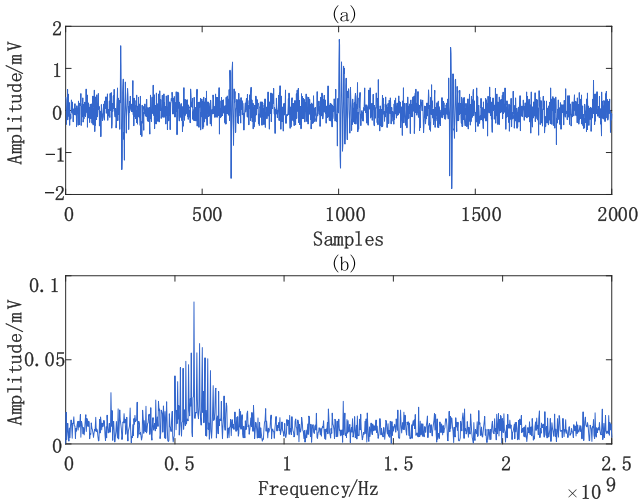

FIGURE 5. (a) Signal with suppressed narrowband noise and its (b) spectrum of denoised signal.

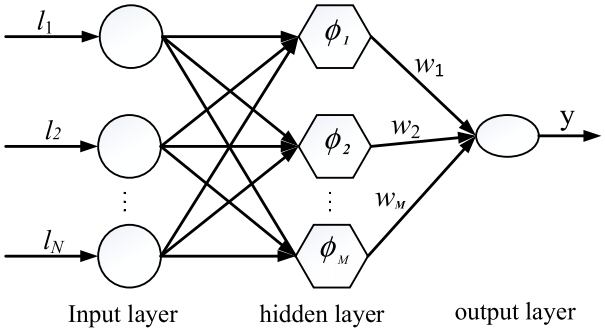

FIGURE 6. The structure diagram of RBF neural network.

window in this paper. The Gaussian function expression is:

$$G = \exp\left[\frac{-(l-\mu)^2}{2\lambda^2}\right] \tag{8}$$

where l is the input vector, μ is the center of the window function and λ is the scale factor.

In order to determine the parameters of the Gaussian window, RBF neural network is used to approximate signal in Fig.5(a), and the Gaussian window is applied to process the approximate signal.

A. EXTRACT PD SIGNAL CHARACTERISTICS WITH RBF NEURAL NETWORK

RBF neural network is a kind of local approximation network, whose Gauss kernel can approximate any continuous function with arbitrary precision under the configuration of weight coefficient, center, width and other parameters. In essence, these parameter spaces can be represented by Gauss kernel to determine the signal, and the least-squares criterion is generally used in training. The mean square error of uncertain random noise signal should be minimized. Usually the measured PD signal is composed of the certain PD signal and the uncertain noise. Therefore, the process described by RBF neural network can be used as a filter. Its three-layer forward network structure model [17] is shown in Fig.6.

Generally, Gauss kernel function is used as the basis function of RBF neural network, and its mathematical expression is as follows:

$$\phi_j(l) = \exp\left(-\frac{\|l-\zeta_j\|^2}{2\eta_j^2}\right), \quad j = 1, 2, \cdots, M \tag{9}$$

where l is the sample with the same length as Fig.6, ζ_j and η_j are the center and width of the j-th element basis function respectively, M is the number of hidden layer nodes. The purpose of network training is to approximate the noiseless PD signal. In the learning sample, the input is the timing sequence of the signal, and the output is the PD signal after suppressing the narrowband noise. According to the least-square theory, the training process is the process of minimizing noise energy:

$$\hat{\Omega} = \arg\min_{\Omega} \sum_{l=1}^{N} \left[\sum_{j=1}^{M} \omega_j \phi_j(l) - y(l)\right]^2 \tag{10}$$

where ω is the network weight from the hidden layer to the output layer, and its cost function is the energy of noise, $y(l)$ represents the output value when the input is l, Ω is the parameter space $\{\zeta_j, \eta_j, \omega_j\}_{j=1\cdots M}$ of the neural network, whose parameters can be obtained by training [18]. $\hat{\Omega}$ is the estimate of Ω. After the training, linearly combine the parameters in the parameter space $\hat{\Omega}$ with the output of the hidden layer according to the network topology, and the PD signal after training can be obtained as follows:

$$y = \sum_{j=1}^{M} w_j * \phi_j(l) \tag{11}$$

In the RBF neural network approximation process, when the rank M of the hidden layer neuron is equal to the sample number of the input, the high degree of network freedom can map the whole noisy signal. When the rank M of neurons is too small, only a few useful signals are obtained due to the low degree of freedom. Therefore, the appropriate rank of hidden layer neurons can effectively distinguish the sample space noise and useful signals. In this paper, a feedback mechanism is designed to determine the rank M of the hidden layer neurons, and the low-rank neurons are obtained only to approximate the useful signals. At this point, the training of RBF neural network achieves the best approximation effect, retains most useful signals, and eliminates a lot of white noise.

The specific steps of RBF denoising are as follows:

Step 1: Input the sample l and the iteration number is set as: $M = 1$.

Step 2: Figure out the output of each hidden layer and output layer.

Step 3: Calculate the error between the output layer and the expected output.

Step 4: Find the parameters with the smallest error and sum them linearly to output y.

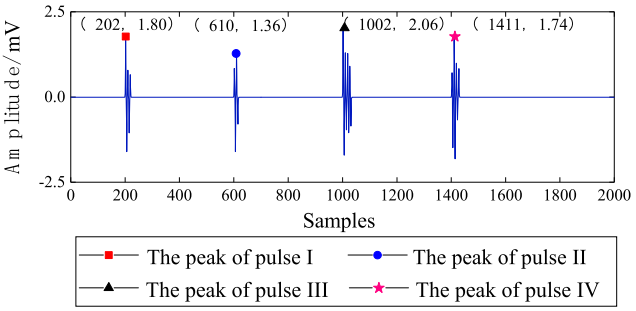

FIGURE 7. Fit result of radial basis function neural network.

TABLE 2. Starting point estimation of pulses.

The starting point of the simulation	The starting point of pulse after RBF neural network training	Approximation rate /%
200	199	99.5
600	599	99.8
1000	999	99.9
1400	1400	100

Step 5: Judge whether there is noise in the output signal y. If there is noise in the output signal y, let $M = M + 1$ and jump to step 3 to continue the cycle. If there is no noise, then output signal y with rank M and terminate the program.

From the above feedback mechanism, when M is 24, the training can best approximate the effective pulse signal. And the result of output is shown in Fig.7. From Fig.7, we can obtain the features of the pulse such as peak position and its starting points.

B. DESIGN OF GAUSSIAN WINDOW AND FILTERING

According to the training results of RBF neural network in Fig.7, the peak position of each pulse is taken as the Gaussian window center μ, and the width of each pulse is taken as the window width λ. From Fig.7, it can be seen that μ is 202, 610, 1002 and 1411, and λ is 24, 20, 36 and 32, respectively. Since the starting point of each pulse is different, it is necessary to estimate the starting points of each pulse in order to obtain more PD signal information. After RBF neural network training, the starting points of pulses are listed in Table 2. Comparing the starting points of simulated PD pulses with that trained by low-rank RBF neural network, they are very close. so we can use the starting points of trained pulses to intercept Gaussian window. Generally, the PD pulses reach the peak and decline. Therefore, the right side lobe of the captured Gaussian window is used to filter the noise signal.

C. WHITE NOISE SUPPRESSION

The concrete steps of the proposed method to suppress white noise are as follows:

Step 1: The method of RBF neural network is used to approximate the noisy signal, and the rank of effective neuron is determined by the feedback mechanism.

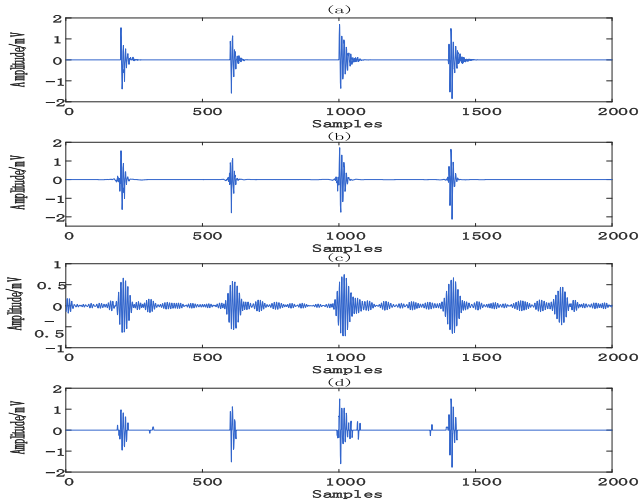

FIGURE 8. (a) PD signal denoised by Gaussian window; (b) Spectrum of the denoised PD signal.

Step 2: According to the best approximation PD signal, the peak and width of pulses are determined.

Step 3: The peak and width of each pulse is taken as the center and width of the Gaussian window respectively. In combination with waveform characteristics, Gaussian window is used to filter noisy signal.

Fig.8 shows the denoised PD signal and its spectrum. From Fig.8(a), comparing the noisy PD signal X_{noise} with denoised PD signal $X_{denoise}$, it can easily observe that the Gaussian white noise has been well suppressed and the effective PD components in original signal have been restored this method.

V. ANALYSIS AND COMPARISON OF DENOISING EFFECT

A. DENOISING THE SIMULATION PD SIGNAL

Three traditional denoising methods are employed to compare with the proposed method, which are as follows. *Method* 1: EDSSV-RBF. *Method* 2: Generalized S-transform and Module Time-Frequency Matrix (S-SVD) [4]. *Method* 3: Adaptive Singular Value Decomposition (ASVD) [13]. *Method* 4: empirical mode decomposition with wavelet transform (EMD-WT) [19]. The simulation is conducted by MATLAB software running in Intel(R) Core (TM) i7-8565U CPU and 8GB RAM. The denoised PD signals by above methods are shown in Fig.9. It can be seen from Fig.9(b) that S-SVD can perform well in denoising, but the starting points of the PD pulses are distorted. In Fig.9(c), the denoising effect of ASVD algorithm is not ideal, as it failed to remove the narrowband noise, resulting in a lot of residual noise. Fig.9(d) shows that after EMD-WT noise reduction, the effective components are lost seriously and slight noise still exists. In comparison with the noise reduction results of above three methods, the presented method shows superior performance in noise suppression and feature preservation, which is conductive to the further analysis of the waveform.

In this paper, the normalized correlation coefficient (*NCC*), root mean squared error (*RMSE*) and signal-noise ratio (*SNR*)

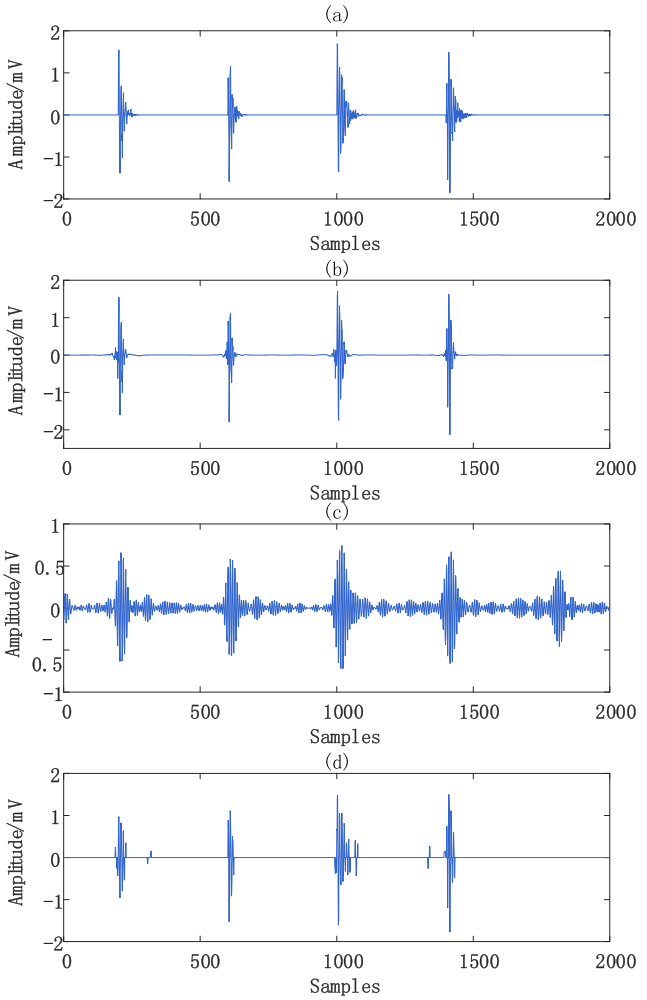

FIGURE 9. Denoising results by different algorithms: (a) Denoised signal by *method* 1; (b) Denoised signal by *method* 2; (c) Denoised signal by *method* 3; (d) Denoised signal by *method* 4.

from literature [20] are used to quantitatively evaluate the denoising performance.

1) The *NCC* is used to describe the similarity of waveform between the original and denoised signal. The *NCC* value is range from -1 to 1. The closer *NCC* to 1, the more similar the waveform is. Which is defined as:

$$NCC = \frac{\sum_{i}^{N} s(i) * x(i)}{\sqrt{\left(\sum_{i=1}^{N} s(i)^2\right) * \left(\sum_{i=1}^{N} x(i)^2\right)}} \tag{12}$$

2) The *SNR* illustrates the effectiveness of noise suppression, which is defined as:

$$SNR = 10 * \log_{10} \frac{\sum_{i=1}^{N} s(i)^2}{\sum_{i=1}^{N} [x(i) - s(i)]^2} \tag{13}$$

TABLE 3. Evaluation parameters of denoising results.

	NCC	*RMSE*	*SNR*
Method 1	0.9992	0.0687	16.52
Method 2	0.9987	0.1000	13.25
Method 3	0.9921	0.0730	15.98
Method 4	0.9985	0.0893	14.24

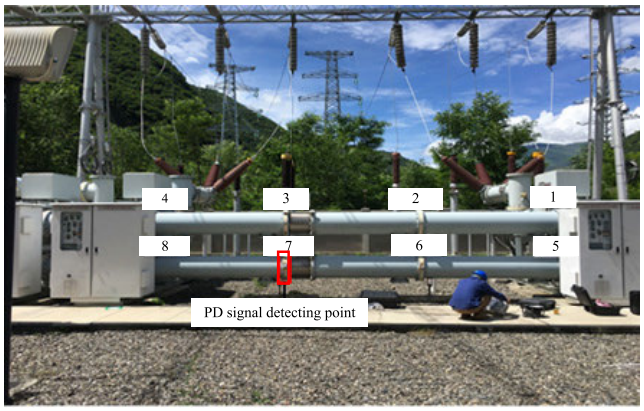

FIGURE 10. Field picture of the PD detection.

3) The *RMSE* is used to evaluate the signal error for the original noiseless and denoised signal, which is defined as:

$$RMSE = \sqrt{\frac{1}{N}\sum_{i=1}^{N}[x(i) - s(i)]^2} \tag{14}$$

where $x(i)$ is the original noiseless PD signal, $s(i)$ is the denoised PD signal, and N is the length of sample.

According to the above evaluation indices, the results of the four methods are listed in Table 3, and we can see that *method* 1 has a better denoise performance than the other three methods, with a higher *SNR* and the best feature retention.

Therefore, the proposed method can detect the field signal, and realize simultaneous suppression of white noise and narrowband noise.

B. PROCESSING FIELD MEASURED PD SIGNAL

To verify the effectiveness of the proposed method, field PD signal was detected from 110kV GIS high-voltage electrical equipment in actual field operation. The picture of the field test is shown in Fig.10, and the sampling rate is 2GSa/s. UHF sensor was employed to detect the PD signal, Fig.11(a) signal was detected at the point 7 in Fig.10. The measured signal can be approximately regarded as non-narrowband noise interference signal, so two narrowband noise are artificial added to the detected signal with an amplitude of 1mV and a frequency of 470Hz and 900Hz respectively. The mixed noise PD signal is shown in Fig.11(b). At this time, the detected PD signal is severely interfered and the feature of useful signal cannot be effectively recognized.

Four methods are employed to deal with the noisy PD signal, and the denoising results are shown in Fig.12. Since the

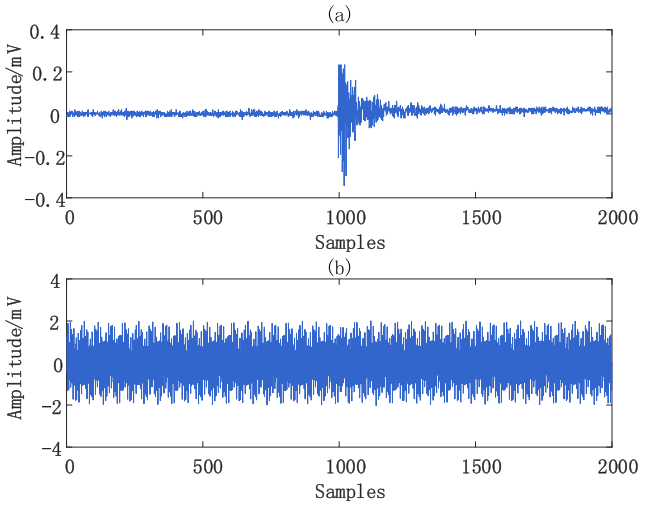

FIGURE 11. PD signal measured in field test.

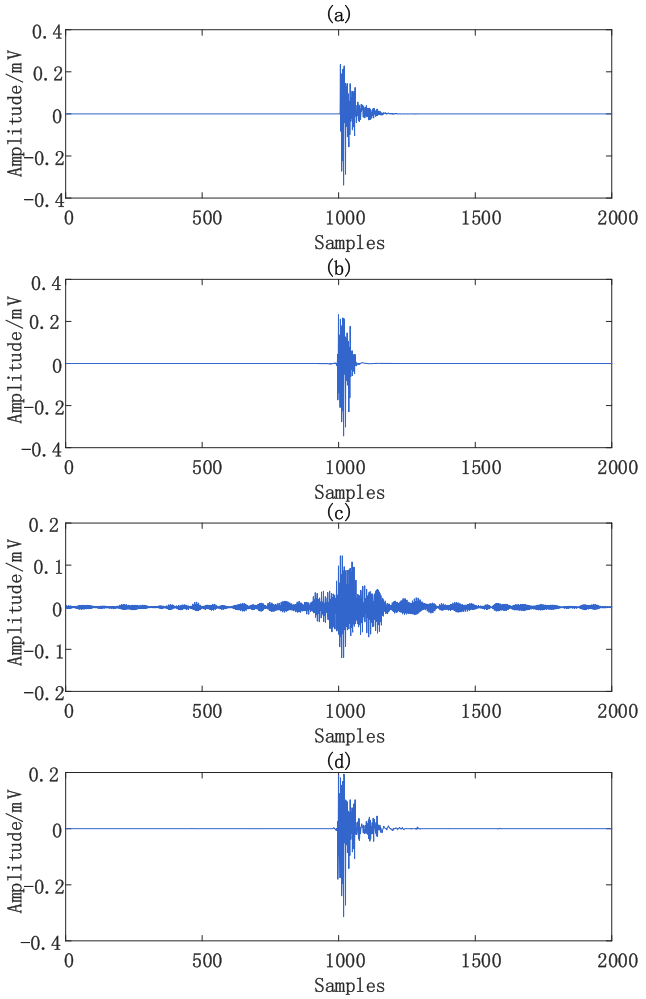

FIGURE 12. Final denoising result by (a) *Method* 1 (b) *Method* 2 (c) *Method* 3 (d) *Method* 4.

pure PD signal cannot be obtained in the field environment, the noise reduction ratio (*NRR*) [21] is used to evaluate the denoising results, which is defined as:

$$NRR = 10 * \left(\log_{10}\sigma_1^2 - \log_{10}\sigma_2^2\right) \tag{15}$$

TABLE 4. Denoising evaluation parameters of measured signals.

Evaluation Parameter	*Method* 1	*Method* 2	*Method* 3	*Method* 4
NRR	16.0221	15.7169	11.9981	15.6047

where σ_1 and σ_2 are the standard deviations of detected signal and denoised PD signal. *NRR* can reflect the results of the denoising, higher *NRR* value is, the higher effective noise suppressing will be.

To compare the EDSSV-RBF with traditional methods, the evaluation indices are computed by equation (15), and the results of the indices are listed in Table 4. The *NRR* of *method* 1 is 16.0221, and the result of denoising is shown in Fig.12(a), the EDSSV-RBF algorithm can effectively suppress noise and extract PD signal. As shown in Fig.12 and Table 4, ASVD algorithm shows weak noise reduction, *NRR* is only 11.9981. The *NRR* value of S-SVD algorithm is slightly higher than EMD-WT algorithm in Table 4. But both of them are lower than EDSSV-RBF algorithm, and the PD signal extraction effect of both of them is not as clean as EDSSV-RBF. In conclusion, the proposed algorithm shows the best performance in denoising and less waveform distortion.

VI. CONCLUSION

In this paper, a novel denoising method based on EDSSV and low-rank RBF neural network is proposed to realize white noise and periodic narrowband noise suppression in PD UHF signals. The effectiveness of the proposed method is verified through the analysis of simulation and field signals. The results are concluded as follows:

1) The energy difference spectrum of singular value can quickly determine the effective rank order of reconstruction matrix, and avoid the influence of human factors.
2) The results of simulation and field detection show that the combination of low-rank RBF neural network and Gaussian window filter can effectively suppress white noise and feature preservation, which is helpful for the subsequent PD signal analysis.
3) Compared with traditional methods, the proposed method is more robust and adaptive, with higher noise suppression ratio. It also better retains the features of original PD pulses, which are of great significance to the on-line monitoring of partial discharge.

REFERENCES

[1] J. Zhang, J. He, J. Long, M. Yao, and W. Zhou, "A new denoising method for UHF PD signals using adaptive VMD and SSA-based shrinkage method," *Sensors*, vol. 19, no. 7, p. 1594, Apr. 2019.

[2] J. Xie, Y. Wang, F. Lv, and M. Li, "Denoising of partial discharge signal using rapid sparse decomposition," *Int. Trans. Electr. Energy Syst.*, vol. 26, no. 11, pp. 2494–2512, Oct. 2016.

[3] G. Li, X. Wang, X. Li, A. Yang, and M. Rong, "Partial discharge recognition with a multi-resolution convolutional neural network," *Sensors*, vol. 18, no. 10, p. 3512, Oct. 2018.

[4] Y. Liu, W. Zhou, P. Li, S. Yang, and Y. Tian, "An ultrahigh frequency partial discharge signal de-noising method based on a generalized S-transform and module time-frequency matrix," *Sensors*, vol. 16, no. 6, p. 941, Jun. 2016.

[5] S. Sriram, S. Nitin, K. M. M. Prabhu, and M. J. Bastiaans, "Signal denoising techniques for partial discharge measurements," *IEEE Trans. Dielectr. Electr. Insul.*, vol. 12, no. 6, pp. 1182–1191, Dec. 2005.

[6] J. Zhong, X. Bi, Q. Shu, M. Chen, D. Zhou, and D. Zhang, "Partial discharge signal denoising based on singular value decomposition and empirical wavelet transform," *IEEE Trans. Instrum. Meas.*, vol. 69, no. 11, pp. 8866–8873, Nov. 2020.

[7] H. Jahangir, E. Hajipour, M. Vakilian, A. Akbari, T. Blackburn, and B. T. Phung, "A method to capture and de-noise partial discharge pulses using discrete wavelet transform and ANFIS," *Int. Trans. Electr. Energy Syst.*, vol. 25, no. 11, pp. 2696–2712, Nov. 2015.

[8] J. Seo, H. Ma, and T. Saha, "Probabilistic wavelet transform for partial discharge measurement of transformer," *IEEE Trans. Dielectr. Electr. Insul.*, vol. 22, no. 2, pp. 1105–1117, Apr. 2015.

[9] Y.-W. Tang, C.-C. Tai, C.-C. Su, C.-Y. Chen, and J.-F. Chen, "A correlated empirical mode decomposition method for partial discharge signal denoising," *Meas. Sci. Technol.*, vol. 21, no. 8, Jun. 2010, Art. no. 085106.

[10] X. Chen and Y. Yang, "Analysis of the partial discharge of ultrasonic signals in large motor based on Hilbert-Huang transform," *Appl. Acoust.*, vol. 131, pp. 165–173, Feb. 2018.

[11] K. Zhou, Y. Huang, M. Xie, M. He, and S. Zhao, "Mixed noises suppression of partial discharge signal employing short-time singular value decomposition," *Trans. China Electrotech. Soc.*, vol. 34, no. 11, pp. 2435–2443, Nov. 2019.

[12] S. Govindarajan, J. Subbaiah, A. Cavallini, K. Krithivasan, and J. Jayakumar, "Development of Hankel-SVD hybrid technique for multiple noise removal from PD signature," *IET Sci., Meas. Technol.*, vol. 13, no. 8, pp. 1075–1084, Oct. 2019.

[13] M. Ashtiani and S. Shahrtash, "Partial discharge de-noising employing adaptive singular value decomposition," *IEEE Trans. Dielectr. Electr. Insul.*, vol. 21, no. 2, pp. 775–782, Apr. 2014.

[14] W.-Y. Chang, "Partial discharge pattern recognition of cast resin current transformers using radial basis function neural network," *J. Electr. Eng. Technol.*, vol. 9, no. 1, pp. 293–300, Jan. 2014.

[15] L. Si, Z.-B. Wang, and G. Jiang, "Fusion recognition of shearer coal-rock cutting state based on improved RBF neural network and D-S evidence theory," *IEEE Access*, vol. 7, pp. 122106–122121, Aug. 2019.

[16] W. Zhang, J. Zhu, Y. Pu, and J. Min, "Application of singular value energy difference spectrum in axis trace refinement," *Sensors Transducers*, vol. 167, no. 3, pp. 55–60, Mar. 2014.

[17] C.-C. Lee, P.-C. Chung, J.-R. Tsai, and C.-I. Chang, "Robust radial basis function neural networks," *IEEE Trans. Syst., Man, Cybern. B. Cybern.*, vol. 29, no. 6, pp. 674–685, Dec. 1999.

[18] N. B. Karayiannis, "Reformulated radial basis neural networks trained by gradient descent," *IEEE Trans. Neural Netw.*, vol. 10, no. 3, pp. 657–671, May 1999.

[19] M.-Y. Lin, C.-C. Tai, Y.-W. Tang, and C.-C. Su, "Partial discharge signal extracting using the empirical mode decomposition with wavelet transform," in *Proc. 7th Asia–Pacific Int. Conf. Lightning*, Nov. 2011, pp. 420–424.

[20] J. Xie, F. Lv, M. Li, and Y. Wang, "Suppressing the discrete spectral interference of the partial discharge signal based on bivariate empirical mode decomposition," *Int. Trans. Electr. Energy Syst.*, vol. 27, no. 10, p. e2407, Aug. 2017.

[21] Y. Xie, J. Tang, and X. Zhang, "Suppressing white-noise in partial discharge measurements part 2: The optimal de-noising scheme," *Eur. Trans. Electr. Power*, vol. 20, no. 6, pp. 811–821, Sep. 2010.

XIAOLI YANG was born in Sichuan, China, in 1995. She received the B.S. degree in biomedical engineering from the Sichuan University of Science and Engineering, in 2018. She is currently pursuing the master's degree with Sichuan University, China. Her research interests include signal processing in power systems, partial discharge, and condition monitoring of power apparatus.

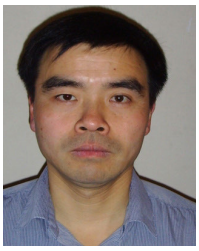

HONGGUANG HUANG received the B.S. degree from the Radio Department, Sichuan University, China, in 1982, and the M.S. degree in communication and electronic systems from Tianjin University, China, in 1985. His research interests include information systems, mobile communication, power telecommunication networks, and signal processing.

QIN SHU (Member, IEEE) received the B.S. (Eng.) degree in power system and automation from Chongqing University, China, in 1982, the M.S. degree in power system and automation from the University of Science and Technology of China, Chengdu, in 1986, and the Ph.D. degree in signal and information processing from the University of Electronic Science and Technology of China, in 1991. His major research interests include modern signal processing, power systems, and condition monitoring of power apparatus.

DAKUN ZHANG was born in 1991. He received the M.S. degree. He is an Engineer with Chengdu Ruichi Technology Company Ltd. His research interest includes the Internet of Things sensing.

BOJIAN CHEN was born in 1989. He received the M.S. degree. He is an Engineer with the State Grid Fujian Electric Power Research Institute. His main research interests include power grid loss analysis, energy conservation and loss reduction, UAV intelligent patrol, and data mining.